AAC Journals.ASM.org

1,4-Azaindole, a Potential Drug Candidate for Treatment of Tuberculosis

Monalisa Chatterji,[a] Radha Shandil,[b] M. R. Manjunatha,[c] Suresh Solapure,[b] Vasanthi Ramachandran,[a] Naveen Kumar,[b] Ramanatha Saralaya,[b] Vijender Panduga,[b] Jitendar Reddy,[b] Prabhakar KR,[b] Sreevalli Sharma,[a] Claire Sadler,[d] Christopher B. Cooper,[e] Khisi Mdluli,[e] Pravin S. Iyer,[c] Shridhar Narayanan,[a] Pravin S. Shirude[c]

Department of Biosciences, IMED Infection, AstraZeneca, Bangalore, India[a]; DMPK and Animal Sciences, IMED Infection, AstraZeneca, Bangalore, India[b]; Department of Medicinal Chemistry, IMED Infection, AstraZeneca, Bangalore, India[c]; Safety Assessment, IMED, AstraZeneca, Alderly Park, Mereside, United Kingdom[d]; Global Alliance for TB Drug Development, New York, New York, USA[e]

New therapeutic strategies against multidrug-resistant (MDR) and extensively drug-resistant (XDR) *Mycobacterium tuberculosis* are urgently required to combat the global tuberculosis (TB) threat. Toward this end, we previously reported the identification of 1,4-azaindoles, a promising class of compounds with potent antitubercular activity through noncovalent inhibition of decaprenylphosphoryl-β-D-ribose 2′-epimerase (DprE1). Further, this series was optimized to improve its physicochemical properties and pharmacokinetics in mice. Here, we describe the short-listing of a potential clinical candidate, compound 2, that has potent cellular activity, drug-like properties, efficacy in mouse and rat chronic TB infection models, and minimal *in vitro* safety risks. We also demonstrate that the compounds, including compound 2, have no antagonistic activity with other anti-TB drugs. Moreover, compound 2 shows synergy with PA824 and TMC207 *in vitro*, and the synergy effect is translated *in vivo* with TMC207. The series is predicted to have a low clearance in humans, and the predicted human dose for compound 2 is ≤1 g/day. Altogether, our data suggest that a 1,4-azaindole (compound 2) is a promising candidate for the development of a novel anti-TB drug.

Studies have revealed that *Mycobacterium tuberculosis*, an opportunistic intracellular bacterium, originated thousands of years ago; genetic analysis of more than 250 contemporary strains indicates its origin with the emergence of *Homo sapiens* in Africa more than 70,000 years ago (1). The spread, evolution, and existence of the bacterium to this day constitute an evolutionary success and a serious threat to humanity (1). Even today, tuberculosis (TB) is a leading cause of mortality in the world, second only to HIV (1). The WHO reported 1.3 million TB-related deaths in 2012 (2). TB has emerged as a global health emergency, as *M. tuberculosis* has acquired resistance to every drug that has been introduced against it (3). Multidrug-resistant (MDR) and extensively drug-resistant (XDR) strains have made TB therapy ineffective, moving treatment of the disease back to the preantibiotic era. The long duration of therapy and associated toxicities have challenged patient compliance and further assisted the development of resistance. A simplified, relatively safe, and shorter-duration therapy is required to combat the TB threat (4). Drugs that work by novel mechanisms, i.e., are active against drug-resistant strains, are urgently needed to treat patients with drug-resistant TB.

M. tuberculosis has a characteristic and complex cell wall architecture involved in multiple functions that are related to cellular physiology and pathogenesis (5). Isoniazid, an important drug in the first-line therapy, inhibits the biosynthesis of mycolic acid, a critical component of the cell wall (6, 7). Ethambutol, another drug in the first-line therapy, also inhibits cell wall synthesis (6, 7). Enzymes that are involved in cell wall biogenesis and/or function have emerged as potential targets for discovery of antimycobacterials; one such target is decaprenylphosphoryl-β-D-ribose 2′-epimerase (DprE1) (6, 7). DprE1, along with DprE2, catalyzes the epimerization of decaprenylphosphoryl-D-ribose to decaprenylphosphoryl-D-arabinose, the sole arabinose donor for cell wall synthesis (8). A number of DprE1 inhibitors that are bactericidal *in vitro* and in a mouse TB infection model have been reported in the literature, building confidence in this target (9–12). Benzothiazinones (e.g., BTZ043), covalent inhibitors of the DprE1 enzyme, have been instrumental in the discovery of the target (9). The nitro group of this scaffold is converted to nitroso, subsequently forming a covalent link with cysteine at position 387 of the enzyme (9). PBTZ, an improved analogue of BTZ043, was shown to be effective in an animal TB model and has a synergistic effect in combination with TMC207 (12). PBTZ is in the preclinical phase of development under the sponsorship of iM4TB (Innovative Medicines for Tuberculosis). TCA1, a noncovalent inhibitor of DprE1, also inhibits MoeW enzymes involved in cell wall and molybdenum cofactor biosynthesis (10). TCA1 is currently in a lead optimization phase that is part of the TB Alliance portfolio [http://www.tballiance.org/downloads/Pipeline/TBA%20Pipeline%20Q1%202014(2)%20(DA).pdf].

We previously reported a novel class of DprE1 inhibitors, 1,4-azaindoles (11). This series emerged from a scaffold morphing

Received 2 May 2014 Returned for modification 26 May 2014
Accepted 18 June 2014
Published ahead of print 23 June 2014
Address correspondence to Monalisa Chatterji, monalisa.chatterji@gmail.com, Radha Shandil, radha.shandil@astrazeneca.com, or Pravin S. Shirude, psshirude@gmail.com.
M.C., R.S., and P.S.S. contributed equally to this work.
Supplemental material for this article may be found at http://dx.doi.org/10.1128/AAC.03233-14.

doi:10.1128/AAC.03233-14
The authors have paid a fee to allow immediate free access to this article.

effort and has demonstrated potent antimycobacterial activity. Members of this class are noncovalent inhibitors of DprE1. In addition, the target site mutations conferring resistance against azaindoles and BTZ043 are distinct from each other. While C387S/G is the primary residue involved in BTZ043 resistance, Y314H imparts resistance to azaindoles. Cross-resistance has not been observed between azaindoles and BTZ043, and azaindoles have been found to be equally active against drug-sensitive and isoniazid/rifampin-resistant strains. A robust understanding of the structure-activity relationship (SAR) has been used to optimize the series.

1,4-Azaindoles possess low molecular weights, low logD values, excellent permeabilities, no CYP inhibition, good oral exposures, low *in vivo* clearance (CL) in rats and dogs and low predicted human CL, and no major safety liabilities as assessed by a spectrum of *in vitro* assays. Moreover, the synthesis of compounds is not complex and is expected to have a low cost. Hence, the 1,4-azaindoles are an attractive class for further development toward TB treatment. During lead optimization, low solubility, high mouse-specific clearance, and weak phosphodiesterase 6 (PDE6) inhibition were mitigated based on an understanding of the SAR of 1,4-azaindoles. This has led to the identification of a potential drug candidate for TB treatment. In this article, the *in vivo* efficacy of the candidate drug in a mouse and rat model of chronic tuberculosis is demonstrated along with its synergy with TMC207. The minimal safety risk (per secondary *in vitro* pharmacology data), the absence of adverse observations during the efficacy study, the drug-like properties, and the acceptable predicted human dosing make 1,4-azaindoles a promising candidate for development.

MATERIALS AND METHODS

Synthesis of selected compounds. (i) *N*-(2-Hydroxyethyl)-1-((6-methoxy-5-methylpyrimidin-4-yl)methyl)-6-methyl-1*H*-pyrrolo[3,2-b]pyridine-3-carboxamide (compound 1). 1-((6-Methoxy-5-methylpyrimidin-4-yl)methyl)-6-methyl-1*H*-pyrrolo[3,2-b]pyridine-3-carboxylic acid (75 mg, 0.24 mmol) was added to dichloromethane (10 ml) to form a suspension. Triethyl amine (66.9 ml, 0.48 mmol) was added, followed by 1-propanephosphonic acid cyclic anhydride (286 ml, 0.48 mmol). The reaction mixture was stirred at room temperature (RT) for 5 min. Ethanol amine (29.0 ml, 0.48 mmol) was added, and the mixture was stirred at RT overnight. After completion of the reaction, the mixture was diluted with dichloromethane (DCM) and was washed with water and brine. The DCM layer was dried over sodium sulfate and evaporated to give the crude product. The crude product was purified by silica gel column chromatography using methanol (MeOH) in DCM to afford *N*-(2-hydroxyethyl)-1-((6-methoxy-5-methylpyrimidin-4-yl)methyl)-6-methyl-1*H*-pyrrolo[3,2-b]pyridine-3-carboxamide as a white solid (compound 1) (yield, 53%).

Electrospray ionization mass spectrometry (ES-MS) *m/z*: 356.4 (M + 1); ^{1}H NMR (300 MHz, dimethyl sulfoxide [DMSO]-d_6) δ ppm: 2.23 (s, 3-H), 2.39 (s, 3-H), 3.39 to 3.65 (m, 4-H), 3.93 (s, 3-H), 4.84 (t, J = 5.09 Hz, 1-H), 5.63 (s, 2-H), 7.74 (s, 1-H), 8.12 (s, 1-H), 8.33 (s, 1-H), 8.41 (s, 1-H), 8.80 (t, J = 5.65 Hz, 1-H).

(ii) 1-((6-(Dimethylamino)-5-methylpyrimidin-4-yl)methyl)-*N*-(2-hydroxyethyl)-6-methyl-1*H*-pyrrolo[3,2-b]pyridine-3-carboxamide (compound 2). To a stirred solution of 1-((6-(dimethylamino)-5-methylpyrimidin-4-yl)methyl)-6-methyl-1*H*-pyrrolo[3,2-b]pyridine-3-carboxylic acid (7 g, 21.51 mmol) in dimethylformamide (DMF) (70 ml), ethanol amine (1.97 g, 32.265 mmol), triethylamine (8.99 ml, 64.53 mmol), and *O*-(7-azabenzo-triazole-1-yl)-1,1,3,3-tetramethyluronium hexafluorophosphate (HATU) (9.81 g, 25.81 mmol) were added, and the mixture was stirred at room temperature for 2 h. Then, the reaction mixture was poured into water (100 ml) and extracted with ethyl acetate (2 × 200 ml). The organic layer was washed with brine and concentrated under reduced pressure. The crude product was purified by silica gel column chromatography using MeOH in DCM to afford 1-((6-(dimethylamino)-5-methylpyrimidin-4-yl) methyl)-*N*-(2-hydroxyethyl)-6-methyl-1*H*-pyrrolo[3,2-b]pyridine-3-carboxamide as a white solid (compound 2) (yield, 60%).

ES-MS *m/z*: 369.4 (M + 1); ^{1}H NMR (400 MHz, DMSO-d_6) δ ppm: 2.27 (s, 3-H), 2.39 (s, 3-H), 2.95 (s, 6-H), 3.45 (q, J = 5.7 Hz, 2-H), 3.54 (q, J = 5.2 Hz, 2-H), 4.81 (t, J = 5.0 Hz, 1-H), 5.52 (s, 2-H), 7.73 (s, 1-H), 8.09 (s, 1-H), 8.22 (s, 1-H), 8.32 (d, J = 1.3 Hz, 1-H), 8.79 (t, J = 5.6 Hz, 1-H).

Microbiology and biochemical assays. Assays to determine the cellular activities (MICs and MBCs), the potency in an intracellular THP1 cell line model, and the IC_{50}s for the DprE1 assay were carried out as described previously (11). The IC_{50} is the compound concentration that results in 50% inhibition of maximal enzyme activity. The MIC refers to the minimal compound concentration that is able to reduce cell growth by ≥80% compared to that of the untreated cells in 7 days, and the MBC refers to the minimal compound concentration that shows a ≥2-log reduction in the number of CFU in 7 days compared to cells at the start of treatment. For MIC determinations, 14 drug-sensitive clinical isolates, 8 isoniazid-resistant (INH^r) strains, and one rifampin-resistant (RIF^r) strain were used.

***In vitro* combination.** The activities of 1,4-azaindole in combination with known anti-TB drugs were determined by the checkerboard titration method (14). Briefly, in a 96-well microtiter plate, one drug was diluted rowwise, and the second drug was diluted columnwise to obtain various combinations of the two drugs in a final volume of 100 μl. Each well of the microtiter plate was inoculated with 100 μl of *M. tuberculosis* H37Rv culture at 5×10^5 CFU/ml. The plates were incubated for 7 days at 37°C. To evaluate whether each paired combination of agents had an additive, synergistic, antagonistic, or indifferent effect in inhibiting *M. tuberculosis*, the fractional inhibitory concentration index (ΣFIC) was calculated using the formula $\Sigma FIC = F_A + F_B$ (F_A is the MIC of drug A in combination/the MIC of drug A alone, and F_B is the MIC of drug B in combination/the MIC of drug B alone).

Synergy was defined as a ΣFIC of ≤0.5, antagonism as a ΣFIC of ≥4.0, and additivity/indifference (no interaction) as ΣFIC values between 0.5 and 4.0.

In a combination of two drugs, indifference equals the effect of the most active component, additivity equals the sum of the effects of the individual components, synergy equals the effect of the combination that exceeds the additive effects of the individual components, and antagonism equals the reduced effect of the combination in comparison with the effect of the more potent individual substance.

All combinations showing a ΣFIC value of <1 were further plated to estimate the numbers of CFU. The $\log_{10}$ CFU reduction in 7 days was calculated with respect to that of the untreated control.

***In vitro* DMPK and safety assays.** *In vitro* DMPK assays to measure aqueous solubility, logD, plasma protein binding, and metabolic stability (mouse/human microsomal intrinsic clearance [CL_{int}]; rat, dog, and human hepatocyte CL_{int}) and safety assays to measure inhibition of the human ether-a-go-go-related gene (hERG) channel, cytochrome P450 enzymes (CYPs), and a panel of ~65 mammalian targets were described earlier (11).

Pharmacokinetics and efficacy in rat and mouse models. Methods used for determining the pharmacokinetics (PK) in mice and rats after intravenous (IVPK) and/or oral administration (POPK) of the drug and the *in vivo* efficacy in mouse and rat models of aerosol infection with TB were described earlier (11, 15). In these models, treatment was initiated after 4 weeks of infection, and the total duration of treatment was 4 weeks (6 days/week). The animals were sacrificed, and viable bacterial counts in their lungs were enumerated.

Pharmacokinetics in dogs. The PK were analyzed in healthy beagles (one male and one female dog per dose group). For intravenous PK (IVPK), a dose of 5 μmol/kg of body weight (BW) of the test compound (compound 1) was administered as a solution containing 5% ethanol, 30% PEG-200, and 65% phosphate-buffered saline (PBS) by infusion. For

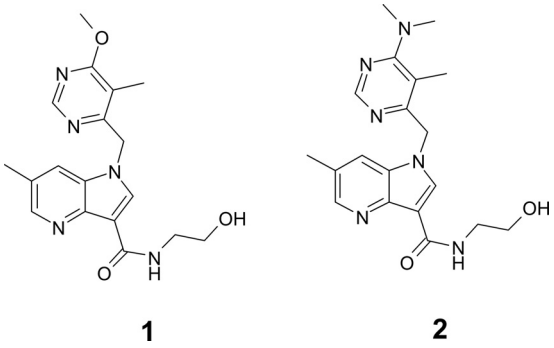

FIG 1 Short-listed compounds from 1,4-azaindole series (compounds 1 [left] and 2 [right]).

oral PK (POPK), 5 μmol/kg of compound 1 was administered in a suspension containing 0.5% hydroxypropyl methylcellulose (HPMC) and 0.1% Tween in water. Blood samples were collected at 5, 10, 20, and 40 min and at 1, 2, 4, 6, and 12 h for IVPK and at 10, 20, and 40 min and at 1, 2, 3, 4, 6, and 12 h for POPK. The blood samples were centrifuged to collect plasma, and the samples were stored at −20°C until analysis using liquid chromatography-tandem mass spectrometry (LC-MS/MS).

Prediction of *in vivo* CL from *in vitro* CL_{int}. Assuming the major route of elimination to be through hepatic metabolism, blood CL in the preclinical species (rat and dog) was predicted from the *in vitro* CL_{int} (by *in vitro-in vivo* correlation [IVIVC]). The *in vitro* CL_{int} was estimated by incubating the test compound with rat or dog hepatocytes. The *in vitro* CL_{int} was scaled to the *in vivo* CL_{int} as follows: CL_{int} *in vivo* = CL_{int} *in vitro* × scaling factors × fu_{blood}/fu_{inc}. The liver weights used for scaling were 40, 32, and 24 g/kg of body weight in rats, dogs, and humans, respectively. The hepatocellularities used for scaling were 163, 169, and 120 cells/g liver (×10^6 cells/g liver) in rats, dogs, and humans, respectively. The free fraction in blood (fu_{blood}) and the unbound fraction in plasma (fu_{plasma}) were assumed to be similar, while the unbound fraction in the hepatocyte mix (fu_{inc}) was predicted using the physicochemical properties (16). The slopes and intercepts from the linear regression analysis of IVIVC for a large number of AstraZeneca compounds were applied for final correction in the scaled *in vivo* CL_{int}. For the prediction of CL, a well-stirred model was used with the following equation: predicted CL = (Q_h × predicted $CL_{int\ in\ vivo}$)/(Q_h + predicted $CL_{int\ in\ vivo}$), where Q_h is the liver blood flow. The values of Q_h are 72, 55, and 20 ml/min/kg in rats, dogs, and humans, respectively (16).

Human dose prediction by allometry. Allometry exponents (*b*) and coefficients (*a*) were estimated by linear regression analysis of a log(CL)-versus-log(body weight [BW]) plot. The equation for simple allometry is $CL = a \times BW^b$.

The steady-state daily area under the concentration-time curve (AUC) required for a 1.0-log_{10} CFU reduction in the rat chronic TB infection model, oral bioavailability (*F* = ratio of dose-normalized AUCs after oral and intravenous [i.v.] administration) in rat, and human CL predicted by IVIVC were used for human dose predictions: predicted human dose = (efficacious AUC in rat × predicted human CL)/*F*.

RESULTS AND DISCUSSION

Selection of potential drug candidates and properties. The 1,4-azaindole series was identified by a scaffold morphing approach as described previously (15). The potency of these compounds against *M. tuberculosis* was mainly improved through the MIC-based SAR with three points of diversification (amide side chain, a hydrophobic group, and core ring substitutions). The secondary amide, referred to as the amide side chain, is essential for potency. It may be involved in the hydrogen-bonding interaction with the target enzyme, DprE1. Small hydrophobic or hydrophilic amides, like methyl cyclopropyl, fluoro-ethyl, or hydroxy ethyl amides, were preferred for lower MICs. The hydrophobic group tolerated various substituted benzyl and heteroaryl-methyl groups; however, monosubstituted benzyl groups were less favored than dis-

TABLE 1 Properties of short-listed compounds from 1,4-azaindole series

Property	Data for compound: 1	2
DprE1 IC_{50} (μM)	0.010	0.032
M. tuberculosis MIC (range) (μM)	0.78–3.12	0.5–1.56
M. tuberculosis MBC (range) (μM)	1.56	1.56–3.12
Drug-sensitive clinical isolate MIC (range) (μM)	0.4–6.25	0.4–3.12
INH^r and RIF^r clinical isolate concn (range) (μM)	0.78–3.12	0.78–1.56
DprE1 overexpression strain MIC (range) (μM)	50–200	200
DprE1 C387S/G (BTZ043) MIC (range) (μM)	0.78–1.56	0.78–1.56
Potency in intracellular THP1 model (log_{10} CFU reduction)	~1.5	~1.5
Cytotoxicity in intracellular THP1 model (μM)	>100	>100
LogD	1.8	1.8
Solubility (μM)	170	464
Mouse properties		
Microsome CL_{int} (μl/min/mg)	28	38
CL_{pred}[a] (ml/min/kg) (% LBF)	16 (11)	28 (18)
Human properties		
Microsome CL_{int} (μl/min/mg)	<4	10
CL_{pred} (ml/min/kg) (% LBF)	4 (19)	6 (30)
Rat properties		
Hepatocyte CL_{int} (μl/min/10^6 cells)	4	5
CL_{pred} (ml/min/kg) (% LBF)	10 (14)	12 (16)
Dog properties		
Hepatocyte CL_{int} (μl/min/10^6 cells)	<1	<1
CL_{pred} (ml/min/kg) (% LBF)	9 (16)	8 (15)
Human properties		
Hepatocyte CL_{int} (μl/min/10^6 cells)	<1	<1
CL_{pred} (ml/min/kg) (% LBF)	2 (9)	2 (11)
fu_{plasma}	0.22	0.30
Caco2 apparent permeability, A to B ($1E^{-6}$ · cm/s)	11	5
CYP[b] inhibition (time-dependent inhibition) (IC_{50} [μM])	>50	>50
hERG IC_{50} (μM)	>33	>33
PDE6 IC_{50} (μM)	4	>100
Secondary pharmacology hits	No significant hits[c]	
Rat PK		
CL (ml/min/kg) (% LBF)	27 (38)	24 (33)
F (%)	100	87

[a] CL_{pred}, predicted clearance.
[b] CYP1A2, CYP2C9, CYP2C19, CYP2D6, and CYP3A4.
[c] In a panel of ~65 high- and medium-severity targets (binding and functional data) (IC_{50}, >100 μM or >30 μM).

TABLE 2 Pharmacokinetic parameters of compounds 1 and 2 in rats and dogs

Compound	Animal model	Hepatocyte CL_{int} (μl/min/10^6 cells)	Measured plasma CL *in vivo* (ml/min/kg)	Predicted blood CL_h (ml/min/kg)	Fold under CL_{pred}
1	Rat	5.8	27	20.6	1.31
	Dog	1	6	8	0.75
2	Rat	4.8	23.7	23.3	1.02

ubstituted benzyl groups. The substitution of a methyl or methoxy group at the C-6 position of the 1,4-azaindole improved cellular potency.

Although 1,4-azaindoles showed excellent *in vitro* and *in vivo* efficacy against *M. tuberculosis*, these compounds had poor aqueous solubility, showed high CL in mice, and weakly inhibited the enzyme activity of host PDE6, which may lead to impaired visual acuity. Therefore, the major focus during lead optimization was to improve these properties while retaining potency against *M. tuberculosis*. The hydroxyethyl amide side chain was crucial for improving aqueous solubility and modulating the physicochemical properties of 1,4-azaindoles. In addition, the hydroxyethyl amide side chain showed a significant improvement in mouse liver microsome (MLM) stability relative to that of hydrophobic amide side chains. The improved MLM stability was attributed to the compounds with lower lipophilicities, as indicated by measured logD values of ≤2. Structurally diverse compounds from the 1,4-azaindole series were profiled for *in vitro* PDE6 screening to understand the PDE6 SAR. The results revealed that the 6-methoxy-5-methylpyrimidine-4-yl group at the hydrophobic pocket was the primary cause of PDE6 activity. It was demonstrated that replacement of the 6-methoxy-5-methylpyrimidine-4-yl substituent with the 6-(dimethylamino)-5-methylpyrimidine-4-yl and 6-(difluoromethoxy)-5-methylpyrimidine-4-yl groups helped to mitigate PDE6 activity.

Thus, from an initial hit, the 1,4-azaindole series was optimized to have molecules with small molecular weights, low logD values, nanomolar DprE1 IC_{50}s, submicromolar MICs, excellent permeabilities, no CYP inhibition, good oral exposures, low clearance in mice, rats, dogs, and humans, and no major safety liabilities. Relatively straightforward synthesis of 1,4-azaindoles with no chiral centers ensures low costs, an essential attribute for an anti-TB drug. The synthesis and characterization of ~250 compounds during lead optimization led to the identification of compound 2 as a potential drug candidate for TB (Fig. 1).

The specific properties of compound 2 along with those of an early tool compound 1 are shown in Table 1. These compounds have logD values of <2, aqueous solubility of >100 μM, similar fu_{plasma} values, nanomolar IC_{50}s against the *M. tuberculosis* DprE1 enzyme, and potent MICs and MBCs against *M. tuberculosis*. These compounds were equally active against drug-sensitive and drug-resistant clinical isolates of *M. tuberculosis*. They were also active against intracellular *M. tuberculosis* and showed ~1.5-log_{10} CFU reductions inside infected THP1 cells (Table 1; see also Fig. S1 in the supplemental material). On the basis of *in vitro* intrinsic clearance (CL_{int}) using hepatocytes from rats and dogs, the predicted *in vivo* clearance (CL) for compounds 1 and 2 ranged between 11% and 30% of liver blood flow (% LBF), indicating low clearance (Table 2). Thus, low CL_{int} in hepatocytes correlated with the observed low CL (<35% LBF) in rats and dogs. Good correlation between the predicted *in vivo* CL and observed *in vivo* CL supported our assumption that hepatic clearance may be the primary route of elimination of these compounds. The IVIVC predicted low CL in humans for the two compounds. High permeability in the Caco2 assay and >85% oral bioavailability in rats and dogs predict excellent bioavailability in humans. Furthermore, TB requires chronic combination therapy; therefore, an understanding of the safety profile is critical. Cytotoxicity assays in THP1 (human monocytic cell line) cells showed no inhibition at up to 100 μM. Compounds 1 and 2 did not inhibit the hERG channel at up to 33 μM concentrations, suggesting a low risk of cardiovascular toxicity. Compounds in this series, including 1 and 2, did not inhibit any of the cytochrome P450 (CYP450) isoenzymes. A panel of mammalian targets associated with serious safety liabilities was used to test for inhibition by 1,4-azaindoles. None of the targets were significantly inhibited except the phosphodiesterase 6 (PDE6) enzyme, which was weakly inhibited by compound 1 (IC_{50}, 4 μM). As described above, the mitigation of PDE6 inhibi-

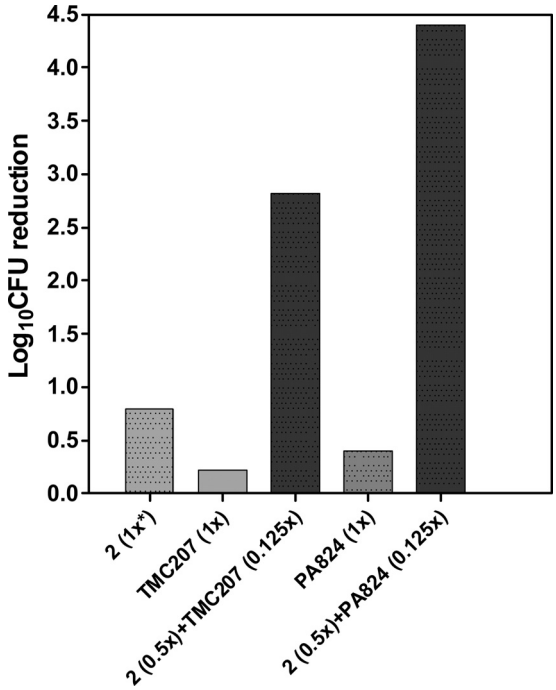

FIG 2 *In vitro* combination study of compound 2 with TMC207 and PA824. For PA824, <200 CFU per ml (limit of quantification) were recovered. Fractional MICs and the F_A and F_B are given in parenthesis for each drug (× indicates fold MIC).

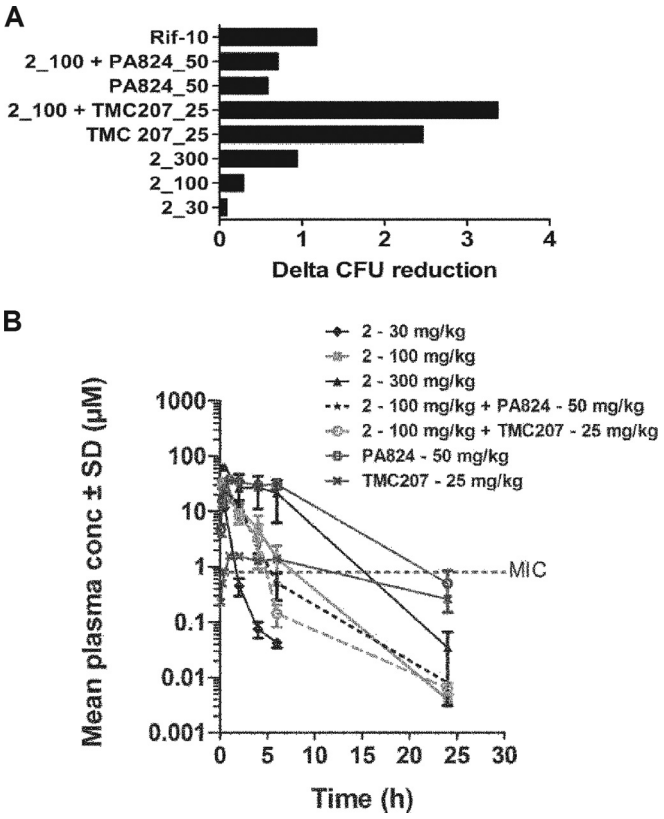

FIG 3 (A) Summary of efficacy of compound 2 alone and in combination with PA824 and TMC207 in a chronic TB infection model in BALB/c mice following 6 days/week oral dosing for 4 weeks. The net $\log_{10}$ CFU/lung reduction was obtained by subtracting lung bacterial counts from that of the vehicle-treated control. Compound 2 exhibited a statistically significant effect at 300 mg/kg versus untreated controls ($P < 0.05$). The mean bacterial counts (± standard deviation [SD]) at the start of treatment (early control) and at the end of treatment (late control) were 6.0 ± 0.08 $\log_{10}$ CFU/lung and 6.24 ± 0.12 $\log_{10}$ CFU/lung, respectively. (B) Time versus concentration profiles of compound 2 and in combination with PA824 and TMC207 following multiple oral administrations at 30, 100, and 300 mg/kg in chronically *M. tuberculosis*-infected mice.

tion (IC_{50}, >100 μM) through systematic medicinal chemistry exploration resulted in the identification of compound 2.

***In vitro* combination study with known TB drugs and clinical candidates.** Compounds 1 and 2 were tested in combination with various first- and second-line anti-TB drugs and clinical/preclinical TB candidates *in vitro*, namely, isoniazid, rifampin, ethambutol, streptomycin, moxifloxacin, imipenem, meropenem, BTZ043, bedaquiline (TMC207), and PA824. Antagonism was not observed for any combination tested in this study. For *M. tuberculosis*, the translation of ΣFIC to bactericidality (reduction in number of CFU) was used to rank order combinations. FIC values were used as a criterion to select combinations for CFU plating. All combinations with a ΣFIC of <1 were plated for an estimation of the reduction in the number of CFU compared to that of individual drugs used at the MIC. Maximum synergy for compound 2 based on the CFU estimate was observed with PA824 and TMC207 (Fig. 2), which was synergistic with PA824 (ΣFIC, 0.5 to 0.625) and additive with TMC207 (ΣFIC, 0.625) based on the FIC.

The combination of compound 2 with TMC207 at sub-MICs showed an additional ~1.5-$\log_{10}$ CFU reduction over the maximum individual drug effect (at the MIC). Similarly, an additional ≥4-$\log_{10}$ CFU reduction was observed with PA824 (Fig. 2). In addition, the combination with meropenem, rifampin, and streptomycin showed weaker synergy with compound 2 (see Fig. S2 in the supplemental material). Similar results were also observed with other compounds from the 1,4-azaindole series described previously (11). Interestingly, BTZ043, which also targets the DprE1 enzyme, exhibited synergy with TMC207 (12, 17). The absence of any antagonism with a variety of tested anti-TB drugs supported the potential of 1,4-azaindoles for combination therapy.

Efficacy and *in vivo* combination study in a mouse model of TB infection. The *in vivo* efficacy of a representative compound (compound 2) was assessed in a BALB/c mouse model of chronic TB infection, wherein the treatment was started on day 28 postinfection. After 4 weeks of treatment with compound 2, the bacterial burden in the lungs was reduced by ~1 $\log_{10}$ CFU/lung at 300 mg/kg of body weight, and statistically significant dose-dependent efficacy was observed (Fig. 3). The oral exposure of compound 2, assessed in infected animals, showed AUCs of 243 μM · h and total plasma concentrations above the MIC for ~15 h at the dose of 300 mg/kg (Table 3). Moreover, compound 2 (at 100 mg/kg) was also tested for *in vivo* combination efficacy with PA824 (50 mg/kg) and TMC207 (25 mg/kg) in the mouse model of chronic TB infection. The bacterial burden in the lungs was reduced by ~0.7 and ~3.5 $\log_{10}$ CFU/lung in combinations with PA824 and TMC207, respectively. Thus, the synergy observed for a 1,4-azaindole (compound 2) with TMC207 (as estimated by CFU reduction) (Fig. 2) *in vitro* translated to *in vivo*. However, this was not true for the combination with PA824. The oral exposure of compound 2, assessed in infected animals, did not change significantly when given in combination with PA824 and TMC207 (Table 3). Similarly, the oral exposures of PA824 and TMC207 remained unchanged when

TABLE 3 Pharmacokinetic parameters of compound 2 following multiple oral dose administrations in *M. tuberculosis*-infected male BALB/c mice[a]

PK parameter[b]	Compound 2			Compound 2 + PA824	Compound 2 + TMC207
Dose (mg/kg)	30	100	300	100 + 50	100 + 25
C_{max} (μM)	25.8 ± 4.1	33.6 ± 5.8	64.9 ± 8.4	26.3 ± 3.6	33.7 ± 3
AUC_{last} (μM · h)	13.4 ± 2.1	65.3 ± 10.7	243 ± 59.1	53.1 ± 7.4	46.3 ± 1.7
T_{max} (h)	0.25 ± 0	0.5 ± 0	0.3 ± 0.1	0.3 ± 0	0.3 ± 0
$t_{1/2}$ (h)	1.2 ± 0.1	2.1 ± 0.2	2 ± 0.4	2.7 ± 0.2	2.8 ± 0.4

[a] Data are means ± SD ($n = 3$).

[b] AUC_{last}, area under the concentration-time curve from time point zero to the time point of the last quantifiable concentration; C_{max}, maximum concentration of drug in serum; T_{max}, time to maximum concentration of drug in serum; $t_{1/2}$, half-life.

TABLE 4 Predicted mean estimates of human CL and dose assuming an oral *F* of 1.0

Compound	Molecular wt	Efficacious dose for ≥1-log CFU reduction in rat model (mg/kg)	Efficacious AUC_{24}[a] in infected rats (μM · h)	Predicted human CL (ml/min/kg)	Predicted human dose (mg/70 kg)
2	368.4	100	166	3.6	925

[a] AUC_{24}, area under the concentration-time curve at 24 h.

these compounds were given in combination with compound 2 (see Fig. S3 in the supplemental material and see Table S1 in the supplemental material). Although streptomycin and meropenem demonstrated synergy *in vitro*, they were not evaluated *in vivo* due to being injectable and due to observed stability issues, respectively. No adverse events were observed during 4 weeks of repeated dosing during the study.

Correlation of CL across species. The pharmacokinetic profile of compound 1 as a representative of the series in mice, rats, and dogs was determined after i.v. and oral dosing. Compound 1 showed oral bioavailabilities of 86% and 100% in rats and dogs, respectively. Interestingly, the observed systemic CL was within 1.5-fold of the predicted value in rats and dogs, confirming the hypothesis that the hepatic route is indeed the primary route of elimination (Table 2). The predicted versus observed *in vivo* CL values were within 1-fold for compound 2 in rats (Table 2). Hence, 1,4-azaindoles showed good *in vitro*-to-*in vivo* correlation. Further, human CL was predicted using IVIVC as described in Materials and Methods. Compounds 1 and 2 were predicted to show low human CL (CL_h, <30% liver blood flow).

Using the observed CL in rats and dogs, the human CL for compound 1 was also predicted by simple two-species (rat and dog) allometry (see Table S2 in the supplemental material). Predicted mean estimates of human CL obtained by allometry (3.3 ml/min/kg) and IVIVC (2.9 ml/min/kg) were very similar. The steady-state daily AUC required for a ≥1.0-log_{10} CFU reduction in a rat model of chronic TB and the predicted human CL predicted ≤1 g per day as an efficacious human dose, assuming complete bioavailability for compound 2 (Table 4). This is a point estimate of the predicted human dose without considering the potential PK variability.

Efficacy study in a rat TB infection model. As described above, a significant challenge associated with the 1,4-azaindole series was rapid metabolism in the presence of mouse liver microsomes. This made it difficult to explore efficacy in the mouse model of tuberculosis for compounds from the 1,4-azaindole series. However, all compounds in the series had low clearances and significant oral exposures in rats. This allowed us to assess representative compounds for *in vivo* efficacy in a rat model of chronic TB infection as an alternative to the well-established mouse model. After 4 weeks of treatment with compounds 1 and 2, the bacterial burden in the lungs was reduced by 0.5 to ≥1 log_{10} CFU/left lobe of the lung, and statistically significant dose-dependent efficacy was observed (Fig. 4). The oral exposures of compounds 1 and 2, assessed in infected animals, showed AUCs ranging from 166 to 240 μM · h, and free

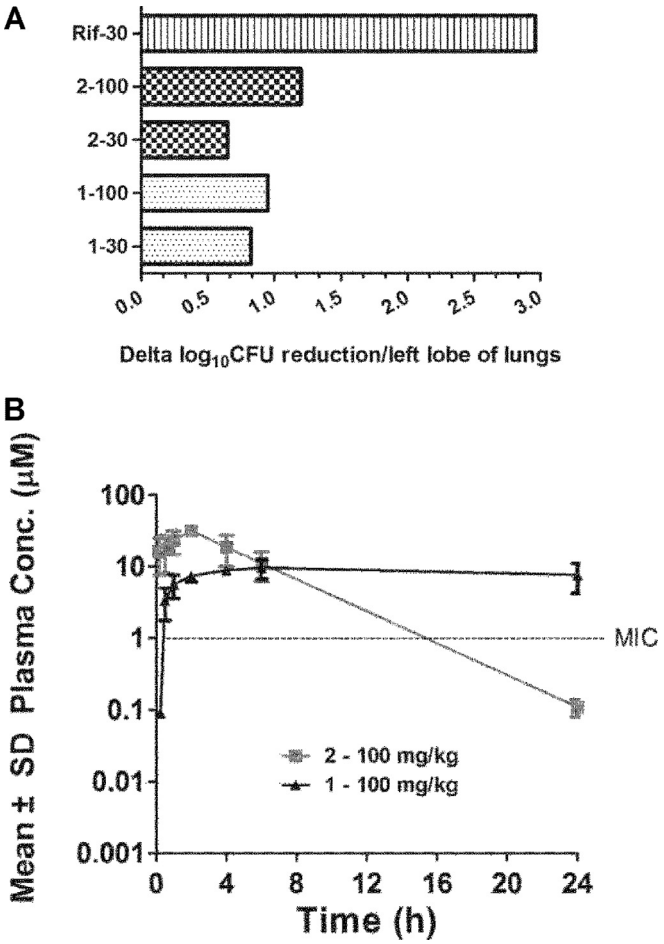

FIG 4 (A) Summary of efficacy of compounds 1 and 2 in a Wistar rat chronic TB infection model following 6 days/week oral dosing for 4 weeks. The net log_{10} CFU reduction/left lobe of the lung was obtained by subtracting bacterial counts from that of the vehicle treated control. Both compounds exhibited a statistically significant effect versus untreated controls ($P < 0.05$). The mean bacterial counts (±SD) at the start of treatment (early control) and at the end of treatment (late control) were 6.02 ± 0.11 log_{10} CFU/lung and 6.41 ± 0.20 log_{10} CFU/lung, respectively. (B) Time versus concentration profiles of compounds 1 and 2 following multiple oral administrations at 100 mg/kg of body weight in chronically *M. tuberculosis*-infected rats.

TABLE 5 Pharmacokinetic parameters of compounds 1 and 2 following multiple oral dose (100 mg/kg) administrations in *M. tuberculosis*-infected male Wistar rats[a]

PK parameter	Compound 1	Compound 2
Dose (mg/kg)	100	100
C_{max} (μM)	46.1 ± 7.7	31.5 ± 3.0
AUC_{last} (μM · h)	986.4 ± 274.3	166.1 ± 43.9
T_{max} (h)	5.3 ± 1.2	2.0 ± 0.0
$t_{1/2}$ (h)	3.8 ± 0.6	4.6 ± 0.0

[a] Data are means ± SD ($n = 3$).

plasma concentrations were maintained above the MIC for 10 to 24 h (Table 5). No adverse events in the form of body weight loss, organ weight loss, or gross pathology were observed following 4 weeks of repeated dosing in the efficacy studies.

In summary, a 1,4-azaindole (compound 2) was identified as a potential clinical candidate for TB treatment. It also showed synergy with TMC207 and no antagonism with other anti-TB drugs.

REFERENCES

1. **Warner DF, Mizrahi V.** 2013. Complex genetics of drug resistance in *Mycobacterium tuberculosis*. Nat. Genet. **45:**1107–1108. http://dx.doi.org/10.1038/ng.2769.
2. **World Health Organization.** 2013. Global tuberculosis report. World Health Organization, Geneva, Switzerland. http://www.who.int/iris/bitstream/10665/91355/1/9789241564656_eng.pdf?ua=1.
3. **Raviglione M, Marais B, Floyd K, Lönnroth K, Getahun H, Migliori GB, Harries AD, Nunn P, Lienhardt C, Graham S, Chakaya J, Weyer K, Cole S, Kaufmann SH, Zumla A.** 2012. Scaling up interventions to achieve global tuberculosis control: progress and new developments. Lancet **379:**1902–1913. http://dx.doi.org/10.1016/S0140-6736(12)60727-2.
4. **Lienhardta C, Vernonb A, Raviglionec MC.** 2010. New drugs and new regimens for the treatment of tuberculosis: review of the drug development pipeline and implications for national programmes. Curr. Opin. Pulm. Med. **16:**186–193. http://dx.doi.org/10.1097/MCP.0b013e328337580c.
5. **Hett EC, Rubin EJ.** 2008. Bacterial growth and cell division: a mycobacterial perspective. Microbiol. Mol. Biol. Rev. **72:**126–156. http://dx.doi.org/10.1128/MMBR.00028-07.
6. **Lu H, Tonge PJ.** 2008. Inhibitors of FabI, an enzyme drug target in the bacterial fatty acid biosynthesis pathway. Acc. Chem. Res. **41:**11–20. http://dx.doi.org/10.1021/ar700156e.
7. **Jackson M, McNeil MR, Brennan PJ.** 2013. Progress in targeting cell envelope biogenesis in *Mycobacterium tuberculosis*. Future Microbiol. **8:**855–875. http://dx.doi.org/10.2217/fmb.13.52.
8. **Mikušová K, Huang H, Yagi T, Holsters M, Vereecke D, D'Haeze W, Scherman MS, Brennan PJ, McNeil MR, Crick DC.** 2005. Decaprenylphosphoryl arabinofuranose, the donor of the D-arabinofuranosyl residues of mycobacterial arabinan, is formed via a two step epimerization of decaprenylphosphoryl ribose. J. Bacteriol. **187:**8020–8025. http://dx.doi.org/10.1128/JB.187.23.8020-8025.2005.
9. **Makarov V, Manina G, Mikusova K, Möllmann U, Ryabova O, Saint-Joanis B, Dhar N, Pasca MR, Buroni S, Lucarelli AP, Milano A, De Rossi E, Belanova M, Bobovska A, Dianiskova P, Kordulakova J, Sala C, Fullam E, Schneider P, McKinney JD, Brodin P, Christophe T, Waddell S, Butcher P, Albrethsen J, Rosenkrands I, Brosch R, Nandi V, Bharath S, Gaonkar S, Shandil RK, Balasubramanian V, Balganesh T, Tyagi S, Grosset J, Riccardi G, Cole ST.** 2009. Benzothiazinones kill *Mycobacterium tuberculosis* by blocking arabinan synthesis. Science **324:**801–804. http://dx.doi.org/10.1126/science.1171583.
10. **Wang F, Sambandan D, Halder R, Wang J, Batt SM, Weinrick B, Ahmad I, Yang P, Zhang Y, Kim J, Hassani M, Huszar S, Trefzer C, Ma Z, Kaneko T, Mdluli KE, Franzblau S, Chatterjee AK, Johnsson K, Mikusova K, Besra GS, Fütterer K, Robbins SH, Barnes SW, Walker JR, Jacobs WR, Jr, Schultz PG.** 2013. Identification of a small molecule with activity against drug-resistant and persistent tuberculosis. Proc. Natl. Acad. Sci. U. S. A. **110:**E2510–E2517. http://dx.doi.org/10.1073/pnas.1309171110.
11. **Shirude PS, Shandil R, Sadler C, Naik M, Hosagrahara V, Hameed S, Shinde V, Bathula C, Humnabadkar V, Kumar N, Reddy J, Panduga V, Sharma S, Ambady A, Hegde N, Whiteaker J, McLaughlin RE, Gardner H, Madhavapeddi P, Ramachandran V, Kaur P, Narayan A, Guptha S, Awasthy D, Narayan C, Mahadevaswamy J, Vishwas KG, Ahuja V, Srivastava A, Prabhakar KR, Bharath S, Kale R, Ramaiah M, Choudhury NR, Sambandamurthy VK, Solapure S, Iyer PS, Narayanan S, Chatterji M.** 2013. Azaindoles: noncovalent DprE1 inhibitors from scaffold morphing efforts, kill *Mycobacterium tuberculosis* and are efficacious *in vivo*. J. Med. Chem. **56:**9701–9708. http://dx.doi.org/10.1021/jm401382v.
12. **Makarov V, Lechartier B, Zhang M, Neres J, van der Sar AM, Raadsen SA, Hartkoorn RC, Ryabova OB, Vocat A, Decosterd LA, Widmer N, Buclin T, Bitter W, Andries K, Pojer F, Dyson PJ, Cole ST.** 2014. Towards a new combination therapy for tuberculosis with next generation benzothiazinones. EMBO Mol. Med. **6:**372–383. http://dx.doi.org/10.1002/emmm.201303575.
13. Reference deleted.
14. **Solapure S, Dinesh N, Shandil R, Ramachandran V, Sharma S, Bhattacharjee D, Ganguly S, Reddy J, Ahuja V, Panduga V, Parab M, Vishwas KG, Kumar N, Balganesh M, Balasubramanian V.** 2013. *In vitro* and *in vivo* efficacy of β-lactams against replicating and slowly growing/nonreplicating *Mycobacterium tuberculosis*. Antimicrob. Agents Chemother. **57:**2506–2510. http://dx.doi.org/10.1128/AAC.00023-13.
15. **Gaonkar S, Bharath S, Kumar N, Balasubramanian V, Shandil RK.** 2010. Aerosol infection model of tuberculosis in Wistar rats. Int. J. Microbiol. **2010:**426035. http://dx.doi.org/10.1155/2010/426035.
16. **Sohlenius-Sternbeck AK, Jones C, Ferguson D, Middleton BJ, Projean D, Floby E, Bylund J, Afzelius L.** 2012. Practical use of the regression offset approach for the prediction of *in vivo* intrinsic clearance from hepatocytes. Xenobiotica **42:**841–853. http://dx.doi.org/10.3109/00498254.2012.669080.
17. **Lechartier B, Hartkoorn RC, Cole ST.** 2012. *In vitro* combination studies of benzothiazinone lead compound BTZ043 against *Mycobacterium tuberculosis*. Antimicrob. Agents Chemother. **56:**5790–5793. http://dx.doi.org/10.1128/AAC.01476-12.